Journal of Fundamental and Applied Sciences

ISSN 1112-9867

Available online at http://www.jfas.info

Research Article

A DFT STUDY OF HYPER-RAYLEIGH SCATTERING (HRS) FIRST HYPERPOLARIZABILITY OF SUBSTITUTED POLYENE: PART (II)

N.S. Labidi

Faculté des Sciences et de la Technologie, Département des Sciences de la Matière,

Université de Tamanrasset.11000, Algérie

Received: 13 September 2021 / Accepted: 02 December 2021 / Published online: 01 January 2022

ABSTRACT

Several DFT functionals have been carried out to study the first hyperpolarizabilities β_{HRS} of push-pull polyene as a function the basis sets, of electron correlation, of the size, of the frequency dispersion and the geometry. These calculations confirm the huge effects of electron correlation, the Møller–Plesset (MP2) results reproduces the values of the first hyperpolarizability obtained with the reference CCSD(T) level. Among density functional theory exchange- correlation functionals, B3LYP, M062X, B3P86 and CAM-B3LYP are comparable to the MP2 for characterizing the dynamic first hyperpolarizability. The TDB3LYP/6-31+G* level show that, as increasing the the separation distance ($d_{N\cdots N}$/Å) and introducing a stronger donor the avereage BLA value decreases and the β_{HRS} increase. In addition, a quantitative relationship was established between the first hyperpolarizability β_{HRS} and the separation distance ($d_{N\cdots N}$/Å) at MP2, B3LYP and M062X level of theory.

Keywords: first hyperpolarizabilities; HRS; D/A Π-conjugated polyene; DFT; MP2.

Author Correspondence, e-mail: labidi19722004@yahoo.fr

doi: http://dx.doi.org/10.4314/jfas.v14i1.12

1. INTRODUCTION

Organic materials with high nonlinear optical response find potential applications in photonic such as active wavelength filters, optical switches, modulators and for terahertz THz wave generation [1–5]. Organic compounds with large delocalized π-electron systems may exhibit extremely larger nonlinear responses, fast electronic response, and the low dielectric constant at optical and radio frequencies compared to the currently studied inorganic materials [3-7].

Progresses to enhance the nonlinear optical NLO properties by designing new compounds are still expected and they rely on a multidisciplinary approach [6-7]. Before addressing the properties of the bulk material, the first step consists in optimizing the molecular responses by finding appropriate interplay between the length and shape of the conjugated segment and the strengths and positions of the donor (D)/acceptor (A) groups [8-9]. Among the recent propositions of such molecular structures, some are based on porphyrin [10], nanotube [11], helicene [12], extended Π-conjugated structures with D/A substituents [13] and Graphyne [14]. The other step aims at translating large molecular responses into large second-order NLO susceptibilities and involves mastering the intermolecular interactions in order to induce proper ordering of the chromophores and electrostatic interactions.

The level of second harmonic generation (SHG) response organic material is intrinsically dependent upon its structural attributes: (i) The degree of charge transfer (CT) across the chromophore determines the intensity of SHG output; (ii) large transition dipole moment;(iii) large excites state with a high charge transfer character.(iv) high asymmetry.(v) a small gap energy between ground and excited state.(vi) High thermal and photonic stability.(vi) planarity, solvent nature and strength of the D-A pair .(vii) the nature of the π-conjugated spacer [8-14].

Following recent work [15], we connect in this study the molecular responses in a series of interesting candidates D-π-NO_2 compounds that have been recently proposed in view of achieving intresting nonlinear optical NLO responses. We address firstly, the methods of calculations of the first hyperpolarizabilities that can be measured using the Hyper-Rayleigh-Scattering (HRS). Secondly, we present DFT and MP2 results, starting with the selection of the best basis set, an assessment of the DFT functionals to correctely evaluate

the first hyperpolarizability, the Π-bridge lengths effects and a description of the frequency dispersion effects as well as of the effects of the solvent. Finally, we discuss structure-property relationships.

2. METHODOLOGY AND COMPUTATIONAL DETAILS

The molecular structures were optimized in vacuum and in acetonitrile solvent at the density functional theory (DFT) level using the B3LYP exchange–correlation functional and the 6-311G* basis set. To take into account the solvent effects the polarizable continuum model within the integral equation formalism (IEF-PCM) [16] was employed at 6-31+G* basis set.

The dynamic $\beta_{HRS}(-2\omega;\omega,\omega)$ and static $\beta_{HRS}(0;0,0)$ first hyperpolarizabilities were evaluated with different schemes. Firstly at the time-dependent Hartree−Fock (TDHF) [17], coupled perturbed Hartree–Fock (CPHF) and secondly at the time-dependent density functional theory (TDDFT) [18]. Only some DFT XC functionals were selected to calculate β: the B3LYP [19], M05-2X and M05 [20], LC-BLYP [21], CAM-B3LYP [22], M062X [23], BHHLYP [24] and B3P86 [25, 26].

Champagne and co-workers [26-28] developed an effective method to evaluate the HRS first hyperpolarizability $\beta_{HRS}(-2\omega;\omega,\omega)$, which is described as:

$$\beta_{HRS}(-2\omega;\omega,\omega) = \sqrt{\left\{\left\langle\beta^2_{ZZZ}\right\rangle + \left\langle\beta^2_{ZXX}\right\rangle\right\}} \qquad (1)$$

$\left\langle\beta^2_{ZZZ}\right\rangle$ and $\left\langle\beta^2_{ZXX}\right\rangle$ are the orientational averages of the molecular β tensor components, which can be calculated using the following equations :

$$\left\langle\beta^2_{ZZZ}\right\rangle = \frac{1}{7}\sum_{\zeta}^{x,y,z}\beta^2_{\zeta\zeta\zeta} + \frac{4}{35}\sum_{\zeta\neq\eta}^{x,y,z}\beta^2_{\zeta\zeta\eta} + \frac{2}{35}\sum_{\zeta\neq\eta}^{x,y,z}\beta_{\zeta\zeta\zeta}\beta_{\zeta\eta\eta} + \frac{4}{35}\sum_{\zeta\neq\eta}^{x,y,z}\beta_{\eta\zeta\zeta}\beta_{\zeta\zeta\eta} + \frac{4}{35}\sum_{\zeta\neq\eta}^{x,y,z}\beta_{\zeta\zeta\zeta}\beta_{\eta\eta\zeta} + \frac{1}{35}\sum_{\zeta\neq\eta}^{x,y,z}\beta^2_{\eta\zeta\zeta} + \frac{4}{105}\sum_{\zeta\neq\eta\neq\xi}^{x,y,z}\beta_{\zeta\zeta\eta}\beta_{\eta\xi\xi} + \frac{1}{105}\sum_{\zeta\neq\eta\neq\xi}^{x,y,z}\beta_{\eta\zeta\zeta}\beta_{\eta\xi\xi} + \frac{4}{105}\sum_{\zeta\neq\eta\neq\xi}^{x,y,z}\beta_{\zeta\zeta\eta}\beta_{\xi\xi\eta} + \frac{2}{105}\sum_{\zeta\neq\eta\neq\xi}^{x,y,z}\beta^2_{\zeta\eta\xi} + \frac{4}{105}\sum_{\zeta\neq\eta\neq\xi}^{x,y,z}\beta_{\zeta\eta\xi}\beta_{\eta\zeta\xi} \qquad (2)$$

$$\left\langle\beta^2_{ZXX}\right\rangle = \frac{1}{35}\sum_{\zeta}^{x,y,z}\beta^2_{\zeta\zeta\zeta} + \frac{4}{105}\sum_{\zeta\neq\eta}^{x,y,z}\beta_{\zeta\zeta\zeta}\beta_{\zeta\eta\eta} - \frac{2}{35}\sum_{\zeta\neq\eta}^{x,y,z}\beta_{\zeta\zeta\zeta}\beta_{\eta\eta\zeta} + \frac{8}{105}\sum_{\zeta\neq\eta}^{x,y,z}\beta^2_{\zeta\zeta\eta} + \frac{3}{35}\sum_{\zeta\neq\eta}^{x,y,z}\beta^2_{\zeta\eta\eta} - \frac{2}{35}\sum_{\zeta\neq\eta}^{x,y,z}\beta_{\zeta\zeta\eta}\beta_{\eta\zeta\zeta} + \frac{1}{35}\sum_{\zeta\neq\eta\neq\xi}^{x,y,z}\beta_{\zeta\eta\eta}\beta_{\zeta\xi\xi} - \frac{2}{105}\sum_{\zeta\neq\eta\neq\xi}^{x,y,z}\beta_{\zeta\zeta\xi}\beta_{\eta\eta\xi} - \frac{2}{105}\sum_{\zeta\neq\eta\neq\xi}^{x,y,z}\beta_{\zeta\zeta\eta}\beta_{\eta\xi\xi} + \frac{2}{35}\sum_{\zeta\neq\eta\neq\xi}^{x,y,z}\beta^2_{\zeta\eta\xi} - \frac{2}{105}\sum_{\zeta\neq\eta\neq\xi}^{x,y,z}\beta_{\zeta\eta\xi}\beta_{\eta\zeta\xi} \qquad (3)$$

In addition, geometric information is given by the depolarization ratio, expressed by (Eq.4):

$$DR = \frac{I_{VV}^{2\omega}}{I_{HV}^{2\omega}} = \frac{\langle \beta_{ZZZ}^2 \rangle}{\langle \beta_{ZXX}^2 \rangle} \qquad (4)$$

For an ideal D/A 1D system DR = 5and for an octupolar molecule DR = 1.5 [28].

The central quantity $\beta_{//}(-2\omega;\omega,\omega)$ corresponds to the projection of the vector part of β on the dipole moment vector:

$$\beta_{//}(-2\omega;\omega,\omega) = \beta_{//} = \frac{1}{5}\sum_i \frac{\mu_i}{||\mu||}\sum_j (\beta_{ijj} + \beta_{jij} + \beta_{jji}) = \frac{3}{5}\sum_i \frac{\mu_i \beta_i}{||\mu||} \qquad (5)$$

where $||\mu||$ is the norm of the dipole moment and μ_i and β_i are the components of the μ and β vectors.

Where $(\beta_{j=1})$ and $(\beta_{J=3})$ are the dipolar and octupolar contributions of the β response, respectively.

$$|\beta_{J=1}|^2 = \frac{3}{5}\sum_{\zeta}^{x,y,z}\beta_{\zeta\zeta\zeta}^2 + \frac{6}{5}\sum_{\zeta\neq\eta}^{x,y,z}\beta_{\zeta\zeta\zeta}\beta_{\zeta\eta\eta} + \frac{3}{5}\sum_{\zeta\neq\eta}^{x,y,z}\beta_{\eta\zeta\zeta}^2 + \frac{3}{5}\sum_{\zeta\neq\eta\neq\xi}^{x,y,z}\beta_{\eta\zeta\zeta}\beta_{\eta\xi\xi} \qquad (6)$$

$$|\beta_{J=3}|^2 = \frac{2}{5}\sum_{\zeta}^{x,y,z}\beta_{\zeta\zeta\zeta}^2 - \frac{6}{5}\sum_{\zeta\neq\eta}^{x,y,z}\beta_{\zeta\zeta\zeta}\beta_{\xi\eta\eta} + \frac{12}{5}\sum_{\zeta\neq\eta}^{x,y,z}\beta^2{}_{\eta\zeta\zeta} - \frac{3}{5}\sum_{\zeta\neq\eta}^{x,y,z}\beta_{\eta\zeta\zeta}\beta_{\eta\zeta\zeta} + \sum_{\zeta\neq\eta\neq\xi}^{x,y,z}\beta_{\zeta\eta\xi}^2 \qquad (7)$$

Then, the nonlinear anisotropy parameter $\rho = |\beta_{J=3}|/|\beta_{J=1}|$ is employed to evaluate the ratio of the octupolar [$\Phi_{\beta J=3} = \rho/(1+\rho)$] and dipolar [$\Phi_{\beta J=1} = 1/(1+\rho)$] contribution to the hyperpolarizability tensor.

To account for frequency dispersion at the Møller–Plesset level MP2 level we employed the multiplicative approximation, which consists in multiplying the MP2 $\beta_{HRS}(0;0,0)$ value by the ratio between the TDHF $\beta_{HRS}(-2\omega;\omega,\omega)$ and CPHF $\beta_{HRS}(0;0,0)$ values. The β is expressed by:

$$\beta_{MP2}(-2\omega;\omega,\omega) \approx \beta_{MP2}(0;0,0) \times \frac{\beta_{TDHF}(-2\omega;\omega,\omega)}{\beta_{CPHF}(0;0,0)} \qquad (8)$$

This approximation, which assumes that frequency dispersion is the same at both the HF and correlated MP2 levels, has been shown to be a satisfactory approximation for different systems [27]. All reported β values are given in a.u. [1 a.u. of $\beta = 3.6213 \times 10^{-42}$ m4 $V^{-1} = 3.2064 \times 10^{-53}$ C^3 m^3 $J^{-2} = 8.639 \times 10^{-33}$ esu] within the T convention. All calculations were

performed using the Gaussian 09 program [29].

3. RESULTS AND DISCUSSION

3.1. Basis set effects

The suitable computational method for the first hyperpolarizabilities of the substituted all trans-hexatriene (Scheme 1), consist on comparing different basis sets (6-31G*, 6-311G*, 6-311G**, 6-31G**, 6-31+G*, 6-311+G*, 6-311+G**, cc-pVDZ, cc-pVTZ, and aug-cc-pVTZ) at the B3LYP level of approximation. The calculated dynamic first hyperpolarizabilities β_{HRS} $\beta_{//}$ and β_{vec} are given in Fig.1.

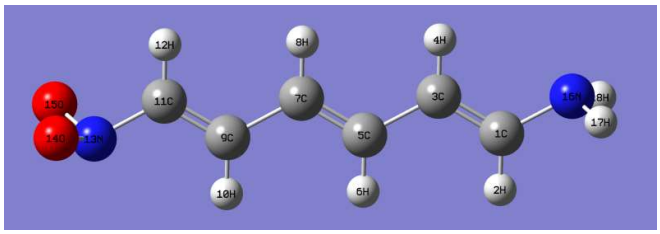

Scheme 1. Structure of the all-trans α,ω-nitro,dimethylamino-Hexatriene.

Fig.1. compares the dynamic first hyperpolarizabilities for substitued hexatriene at differents basis sets. The consequence of polarization functions is seen very clearly, d-polarization functions tend to decrease in the dynamic first hyperpolarizabilities, whereas the p-polarization functions leads to smaller changes. Going from a double-ζ to a triple-ζ basis set leads an increase but not dramatic on hyperpolarizabilities. When adding diffuse functions this always leads to an increase in β_{HRS} $\beta_{//}$ and β_{vec} values.

The results obtained using the aug-cc-pVDZ ,cc-pVDZ and cc-pVTZ basis sets reproduces approximately the TDDFT results. It can be said that diffuse and polarization functions lead to opposite trends for β_{HRS} $\beta_{//}$ and β_{vec}. The choice of an appropriate basis set for the prediction of NLO properties was critically addressed by many authors [5-13]. The common consensus is that the basis set must contain polarization and diffuse functions for the reliable estimation of β_{HRS}. From these results, it is clear that the 6-31+G* and 6-311+G* basis sets were found to be more than adequate for obtaining consistent trends for first hyperpolarizabilities values.

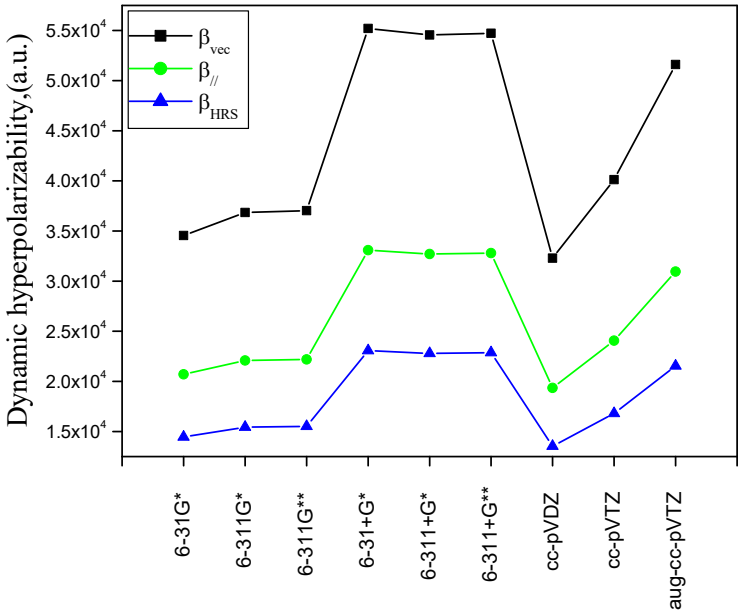

Fig.1. Basis sets effects on the dynamic hyperpolarizability: β⁄⁄, β_{vec} and β_{HRS} of the all trans α,ω-nitro,dimethylamino-hexatriene determined at the B3LYP level.

3.2. Assessment of the DFT functionals to evaluate the first hyperpolarizability

A reliable prediction of first hyperpolarizability β_{HRS} values requires accounting for electron correlation effects. To take into account these effects, calculations were carried out by using the second-order Møller-Plesset (MP2) approximation as a reference method and the DFT approaches with the conventional exchange correlation (XC) functionals (LC-BLYP, B3LYP, B3P86, CAM-B3LYP, M052X, M05, M062X, BHandHLYP). The proposed methods provides first hyperpolarizability values in accord with the CCSD(T) and MP4 results [30].

The results given in Figures (2a and 2b), highlight the impact of the electron correlation on the assessment of hyperpolarizabilities β// and β_{HRS} and depolarization ratio (DR) for isolated all trans α, ω-nitro, dimethylamino-hexatriene using 6-31+G* basis set. **(i)** As shown in Fig.2a, the electron correlation effects are much larger for the static hyperpolarizabilities surrounded by an MP2/HF ratios close to 2.39 and 2.55 for β_{HRS} and β// in succession; **(ii)** The electron correlation effects as estimated using the SCS-MP2 scheme is even larger and amount to an increase of β_{HRS} by 95.39 %. Then, the difference between MP2 and SCS-MP2 is of 2.88%

only; **(iii)** At the DFT approach when going from M062X to LC-BLYP electron correlation leads to an increase of β_{HRS} by 35 to 198% .However, the LC-BLYP functional behaves badly, leading to an overestimations of the HRS first hyperpolarizability, the LC-BLYP functional leads to the highest increase of β_{HRS} by 198% and the smallest ratio with β^{HRS}(MP2)/β^{HRS} (LC-BLYP) close to 0.34, whereas it is often ranging β^{HRS}(MP2)/β^{HRS} (X) between 1.54 and 1.87 for the others DFT approaches. So, the electron correlation effects might be much different from one exchange correlation (XC) functional to another. This statement is also verified for analogous DFT approaches: β_{HRS}(MP2)/β_{HRS} (M05) = 1.865 > β_{HRS}(MP2)/β_{HRS} (BHandHLYP) = 1.738 > β_{HRS}(MP2)/β_{HRS} (B3P86) = 1.736 > β_{HRS}(MP2)/β_{HRS} (B3LYP) = 1.728 > β_{HRS}(MP2)/β_{HRS} (M052X) = 1.617> β_{HRS}(MP2)/β_{HRS} (CAM-B3LYP) = 1.579> β_{HRS}(MP2)/β_{HRS} (M062X) = 1.542.

The values obtained at the MP2 level of theory appear to be in better agreement with the calculated M062X, CAM-B3LYP and M052X functionals, the ratios is rather small. However, slightly worse agreement is obtained for the B3LYP, B3P86, M05 and BHandHLYP functionals, even though LC-BLYP method show more significant overestimation of the β_{HRS}. The β_{HRS} predicted by CAM-B3LYP, M05-2X and BH&HLYP are almost the same and are comparable with those obtained by MP2 method; **(iv)** It is also interesting to point out that the DR ranges from 4.40 to 4.93 within the approximation level, whereas MP2 and SCS-MP2 methods produce a typical linear (D-Π-A) dipolar compounds close to 5. However the HF method generates the lowest value of 4.17. The DR (SCS-MP2)/DR (HF) and DR (MP2)/DR (HF) are both close to 1.18 and the ratio between the references methods DR (SCS-MP2)/DR (MP2) is close to 1.01; **(v)** The electron correlation effects on β// (parallel) for both MP2 and DFT levels are very important it leads for higher increase with an effect factor ranging β// (MP2)/ β//(X) from 0.34 for LC-BLYP to 2.55 for HF, also the ratio between references β//(MP2)/ β// (SCS-MP2) is close to 0.97.

At 6-31+G* basis set the electron correlation effects produce the same behaviour trend for β_{HRS} and $\beta_{//}$. Indeed, the β// (parallel) presents the highest value $\beta_{//}$ =23673a.u. at LC-BLYP; **(vi)** For dynamic (λ = 1064 nm) hyperpolarizability in Fig.2b, the best estimate for the β_{HRS} value of the isolated species amounts to 9710 and 9997a.u. for MP2 and SCS-MP2 level,

respectively. The situation is different when considering XC functional where the LC-BLYP functional behaves poorly, leading to underestimations of the β_{HRS}. It is also interesting to note that the LC-BLYP β_{HRS} values are intermediate between the HF and MP2 results. However, comparison with MP2 results demonstrates that the LC-BLYP functional is unreliable for estimation of the molecular first hyperpolarizability. Conversely much better agreement is observed for the B3LYP functional and B3P86 both appear to behave in a similar manner the β_{HRS}(MP2)/ β_{HRS} (B3LYP) = 1.14 and β_{HRS}(MP2)/ β_{HRS} (B3P86) = 1.17.

The contrasts between the dynamic and static HRS first hyperpolarizability are quantified using the β_{HRS}(1046nm)/β_{HRS} (∞) ratio ranging from 0.44 for LC-BLYP, 1.74 for MP2 and SCS-MP2, 2.24 for M062X, 2.22 for M052X, 2.57 for M05 and 2.63 for B3LYP, the same trend was observed for β// with $\beta_{//}$ (1046nm)/ $\beta_{//}$ (∞) ranges from 0.44 to 2.68. The β_{HRS} predicted by B3LYP, B3P86 and M062X are almost the same and are comparable with those obtained by MP2 method. In addition, results obtained for depolarization ratio DR (dynamic;1046nm)/DR (static;∞) appear to be close to 1.00.

We can conclude that the calculated static and dynamic HRS first hyperpolarizability for all trans α, ω-nitro, dimethylamino-hexatriene indicates that HF underestimates hyper-polarizabilities values comparatively to the accurate MP2 method. However, the difference in the β_{HRS} values for DFT and MP2 does not vary significantly, except the worst functional LC-BLYP which is not recommended for such systems. Consequently, we propose scaling HF hyperpolarizabilities for linear D-π-A molecules by 2.39 and 1.99 to obtain the MP2 at a low computational cost for solvated (acetonitrile) and isolated molecule respectively.

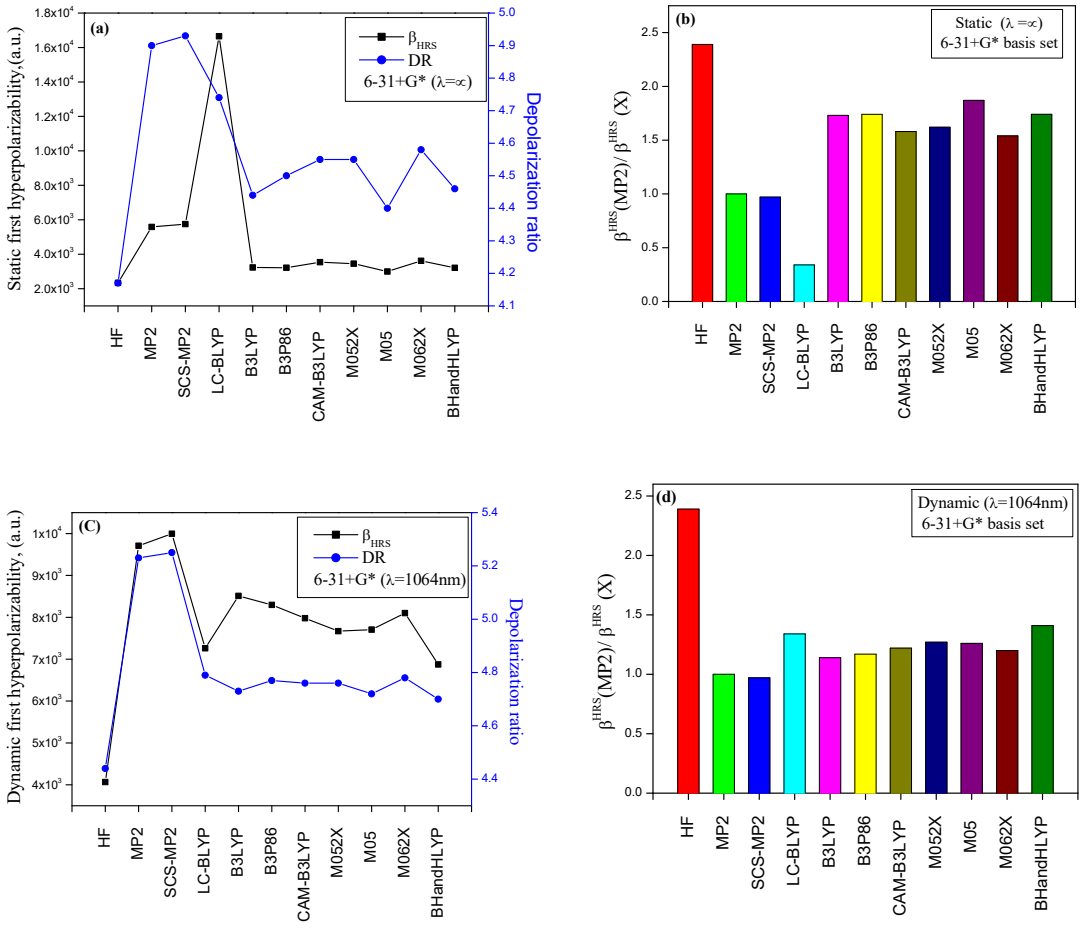

Fig.2. Electron correlation Effects on static and dynamic HRS first hyperpolarizability and depolarization ratio (a and c); β_{HRS} contrasts for all trans α, ω-nitro, dimethylamino -hexatriene calculated at different levels of approximation at 6-31+G* basis set (b and d).

3.3. Effect of bridge length

In Fig.3, we present the β_{HRS} and depolarization ratio (DR) dependence onto separation distance ($d_{N...N}$;Å) between NO_2/$N(Me)_2$ end groups for a series of all-trans α,ω-nitro, dimethylamino-polyene [NO_2-$(CH=CH)_N$ -$N(Me)_2$] (Scheme 2). In Fig.3a and Fig.3b, we present the effect of bridge length between the -NO_2/-$N(Me)_2$ end groups on the dyanamic and static first hyperpolarizability for all trans α,ω-nitro, dimethy- lamino - hexatriene in vaccuo and in acetonitrile within TDHF, TDDFT and MP2 methods by employing the 6-31+G* basis set.

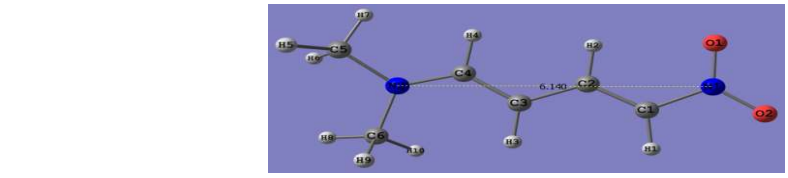

N=2

N=3

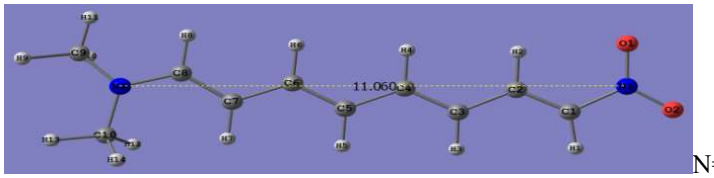

N=4

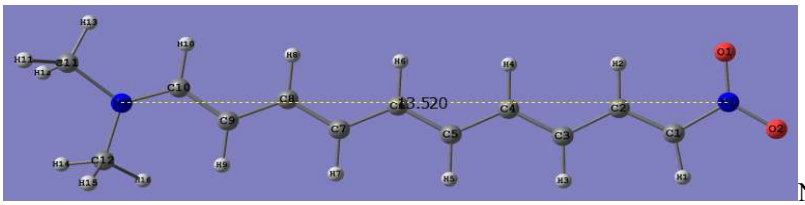

N=5

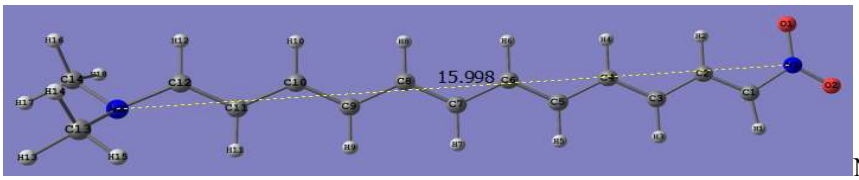

N=6

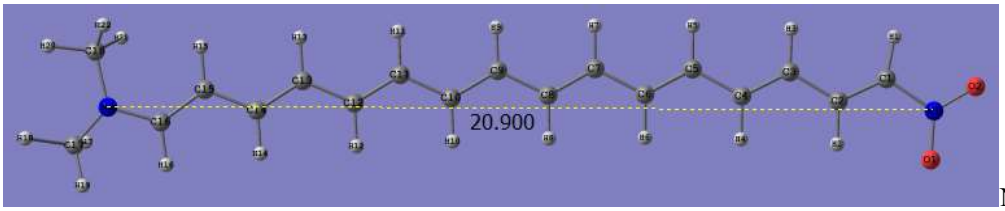

N=8

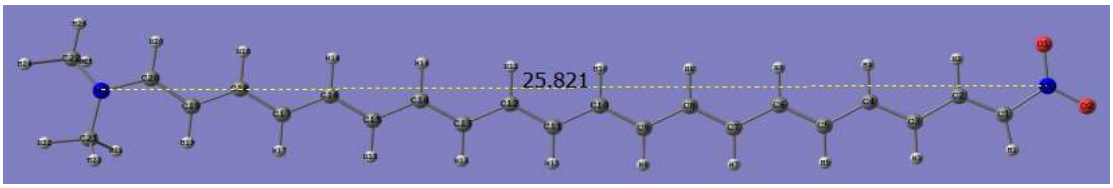

N=10

Scheme 2. Separation distance ($d_{N\cdots N}$/Å) calculated at B3LYP/6-311G* level for substituted polyene NO_2-[(CH=CH)]$_N$-N(Me)$_2$ in acetonitrile solvent.

In general, the first hyperpolarizability β_{HRS} has an uptrend with increasing the separation distance ($d_{N...N}$) in the all trans α,ω-nitro,dimethylamino-hexatriene molecule. The dynamic β_{HRS} (λ = 1064 nm) in acetonitrile increases even more rapidly than in vacuum with increasing the separation distance ($d_{N...N}$) between the two end groups $NO_2/N(Me)_2$. The static first hyperpolarizability β_{HRS} in vacuum and in acétonitrile solvent, appears to be linearly dependent on the $NO_2/N(Me)_2$ $d_{N...N}$ separation distance. However, the dynamic β_{HRS} grow exponentially with the substituted polyene length. The comparison reveals that the solvent effect considerably enhances the HRS hyperpolarizabilities, the quantified solvent effect ratio ($\beta_{HRS}^{sol}/\beta_{HRS}^{vac}$ = 2 to 4) range from 2 for a separation distance of $d_{N\cdots N}$ = 6.1Å to 4 for $d_{N\cdots N}$ = 25.8Å. In addition, since depolarization ratio is about unity ($DR^{sol}/DR^{vac}\sim$ 1.00), one can say that acetonitrile solvent has little effect on DR.

The results obtained by the standard HF are compared with the performances of two different density functionals, namely B3LYP and M06-2X. The HF/6-31+G* calculated HRS first hyperpolarizability turn out to be smaller than the corresponding DFT generated with B3LYP /6-31+G* and M06-2X /6-31+G* functional. Fig.3a and Fig.3b reveals that the static (λ=∞) and dynamic (λ=1064nm) hyperpolarizabilities β_{HRS} evolution with the $d_{N...N}$ separation distance is much steeper at M06-2X and LC-BLYP /6-31+G* levels. For the solvated (acetonitrile) molecule the dynamic first hyperpolarizability HRS reported to the number of double bonds increases exponentially with *N*. Indeed, β_{HRS} (LC-BLYP, 6-31+G*)/*N* amounts to 2420 and 37364 a.u. for N=3 and N=10 and to 7689 and 156670 a.u. in vaccuo and considering acetonitrile solvent, respectively. For the solvated (acetonitrile) β^{1064}_{HRS} (B3LYP)/ β^{1064}_{HRS} (HF) ratio ranges between 1.76 and 2.45 and the β^{1064}_{HRS} (M06-2X)/ β^{1064}_{HRS} (HF) ratio ranges between 1.71 and 10.0. The HF/6-31+G* and B3LYP /6-31+G* functional predict the same evolution trend for the dynamic β_{HRS} obtained in vacuum, they displays an exponentially dependence on the substituted polyene length.

To provide a mathematical model for hyperpolarizability variation, the results obtained by the HF and DFT methods are compared with the MP2 technique for the solvated all-trans α,ω-nitro,dimethylamino-polyene molecules (Fig.4).

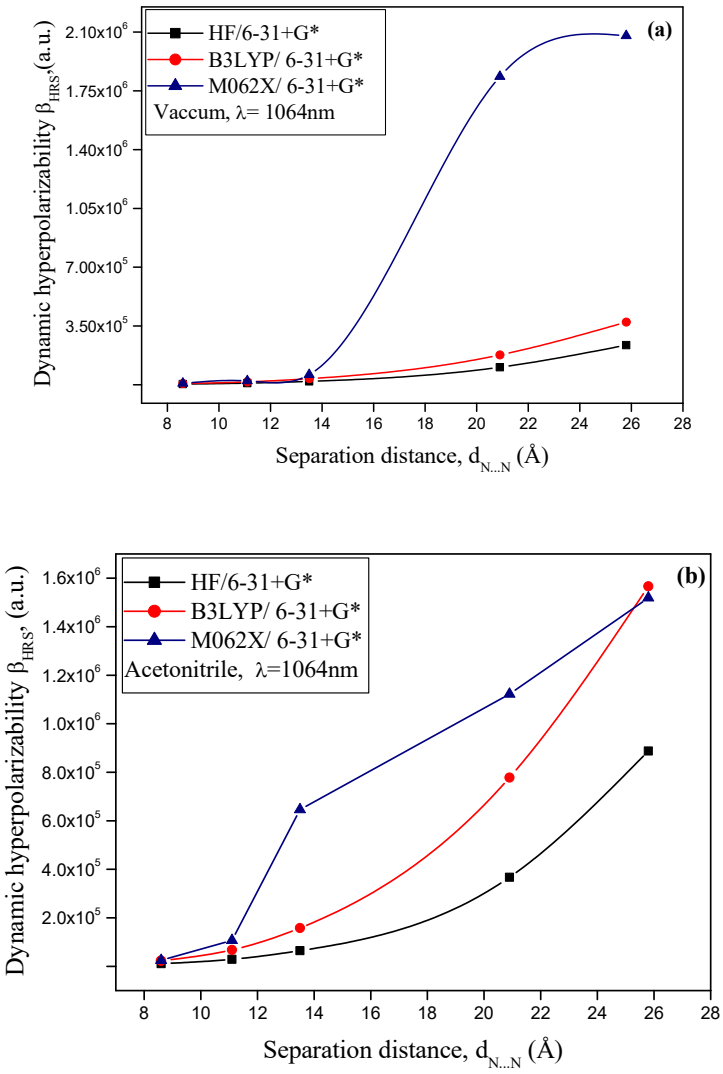

Fig.3. Dynamic β_{HRS} of all trans α,ω-nitro,dimethylamino-hexatriene determined at different levels of theory in vaccuo (a) and considerins acetonitrile solvent(b).

According to the HF and DFT methods used in this investigation, the static hyper-polarizability β_{HRS} displays the linear dependence with the donor-acceptor $N(Me)_2/NO_2$ separation distance at HF/6-31+G*, LC-BLYP /6-31+G* and M06-2X /6-31+G* levels Figures (4a, 4c and 4e), while the dynamic ones (λ = 1064nm) appears to grow exponentially, excepted for the M06-2X / 6-31 + G* functional whose hyperpolarizability in acetonitrile and in vacuum develops a three-order polynomial and power fitting Figures (4b,4b and 4f). Also, the HF calculated HRS first hyperpolarizability for the solvated (acetonitrile) molecule turn out to be smaller than the corresponding MP2 method generated

at the same 6-31+G*basis set. Fig.4g reveals that at MP2/6-31+G* level the growth of static (λ=∞) and dynamic (λ=1064nm) β_{HRS} with the $d_{N...N}$ separation distance are much steeper. The MP2 method always shows the highest increase of β_{HRS} when going from molecules with shorter π-bridges to molecules with longer π-bridges. The MP2/6-31+G* first hyperpolarizabilities β_{HRS} reported to the number of double bonds increases exponentially with *N*. Indeed, β_{HRS} (MP2, 1064nm)/*N* amounts to 7221 a.u. and 113941 a.u. for N=3 and N=10 and the static β_{HRS} (MP2, ∞)/N(3-10) to 6229 a.u. and 14981 a.u. in that order. On the other hand, electron correlation effects lead to the increase of β_{HRS} by about a factor of 2. The gas-phase first hyperpolarizabilities ratios of MP2 to HF β_{HRS}(MP2)/β_{HRS} (HF) are nearly constant and ranges between 2.00 and 1.28 for a separation distance of 8.6Å and 25.8Å respectively. The following relations have been obtained at HF, DFT and MP2 levels:

HF/6-31+G*

Static (λ = ∞)

β_{HRS} = – 41731.31 + 6104.91× $d_{N...N}$ (Acetonitrile, R= 0.99)

β_{HRS} = –15652.54 + 2048.01 ×$d_{N...N}$ (Isolated, R= 0.98)

Dynamic (λ = 1064nm)

β_{HRS} = 1031 exp (0.274 × $d_{N...N}$) (Acetonitrile, R= 0.99)

β_{HRS} = 463.3exp (0.252 × $d_{N...N}$) (Isolated, R=0.99)

B3LYP/6-31+G*

Static (λ = ∞)

β_{HRS} = – 44716.60 + 7693.19× $d_{N...N}$ (Acetonitrile, R= 1.00)

β_{HRS} = – 20071.17 + 2732.83×$d_{N...N}$ (Isolated, R= 0.99)

Dynamic (λ = 1064nm)

β_{HRS} = 2282exp (0.270 × $d_{N...N}$) (Acetonitrile, R= 0.97)

β_{HRS} = 858.4exp (0.248 × $d_{N...N}$) (Isolated, R=0.98)

M062X/6-31+G* level

Static (λ = ∞)

β_{HRS} = – 183467.94 + 22902.60 × $d_{N...N}$ (Acetonitrile, R= 0.98)

β_{HRS} = – 41275.98 + 4988.18 × $d_{N...N}$ (Isolated, R= 0.97)

Dynamic (λ = 1064nm)

β_{HRS} = – 243.06× $(d_{N...N})^{3}$ + 11886.80× $(d_{N...N})^{2}$ – 92060.53× $(d_{N...N})$ + 136345.88 (Acetonitrile, R= 0.99)

$\beta_{HRS} = 0.154\times (d_{N...N})^{5.112}$ (Isolated, R= 0.99)

MP2/6-31+G*

Static (λ = ∞)

β_{HRS} = 175.12× $(d_{N...N})^{2}$ + 1667.93× $(d_{N...N})$ – 9711.43 (Isolated, R= 1.00)

Dynamic (λ = 1064nm)

β_{HRS} = 4208.66× $(d_{N...N})^{2}$ –79986.66× $(d_{N...N})$ + 401402.56 (Isolated, R= 1.00)

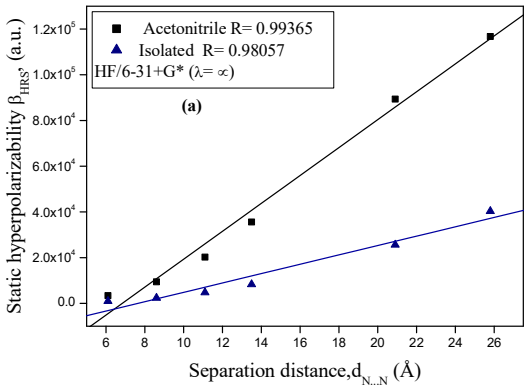

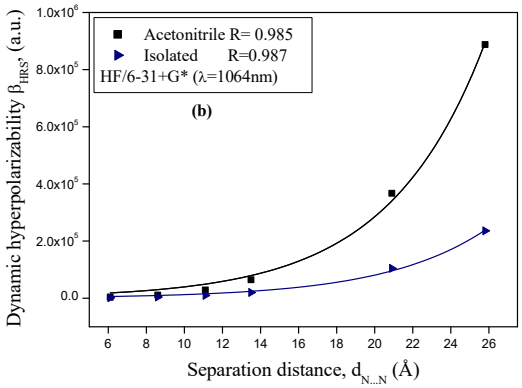

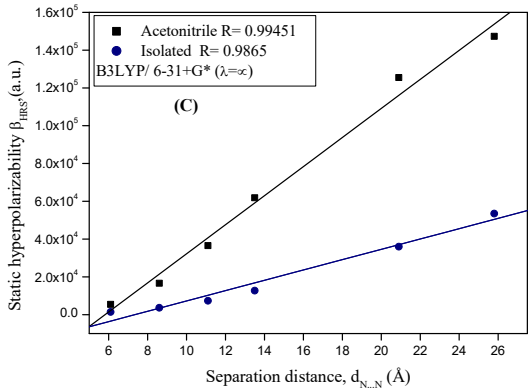

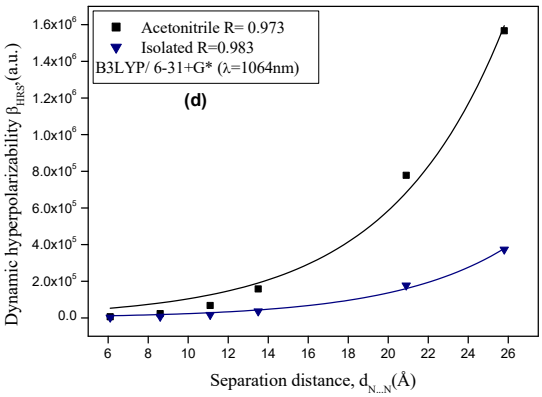

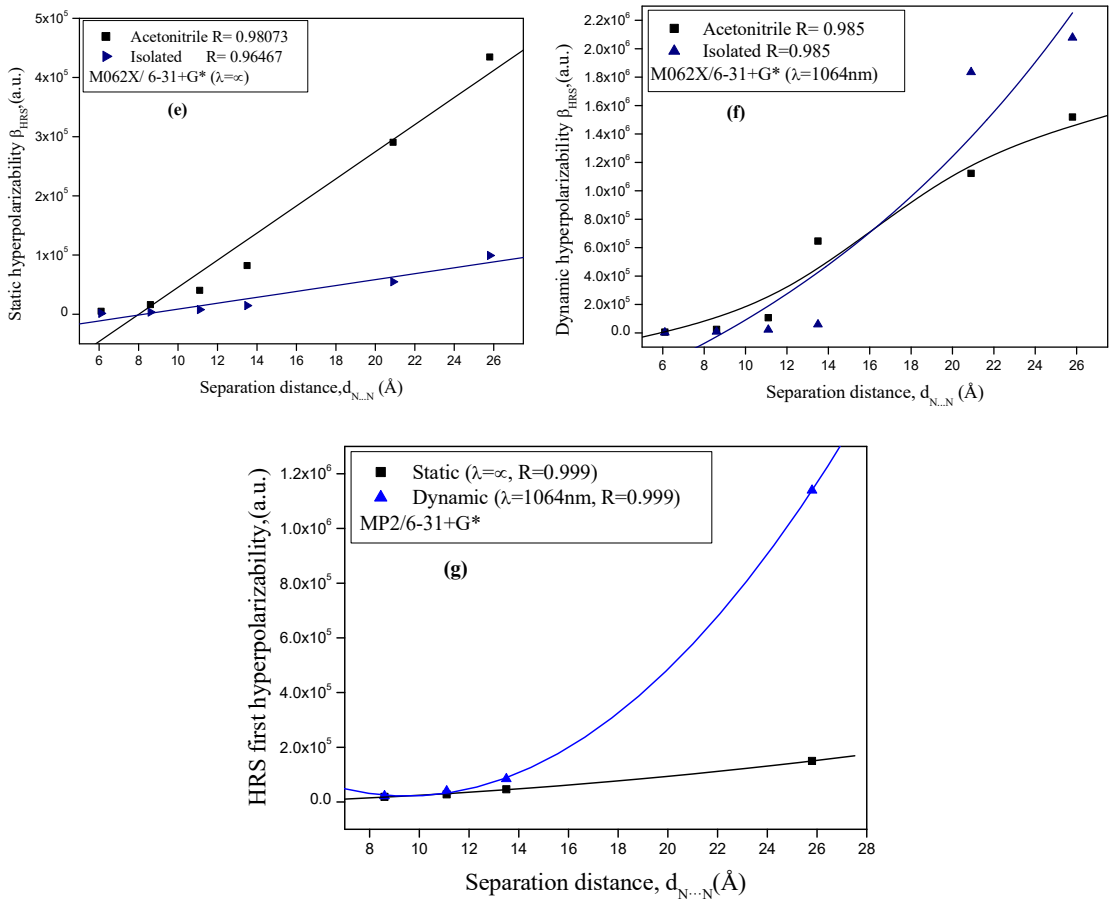

Fig.4. Dependence of the static(λ=∞) and dynamic (λ=1064nm) HRS hyperpolarizability as function of ($d_{N...N}$) separation distance, calculated in vaccuo and acetonitrile according to (a and b) HF, (c,d,e and f) DFT and (g) MP2 methods.

3.4 Frequency dispersion effects

The dynamic perturbations were added in order to explore the effect of frequency dispersion. For comparison, fundamental optical wavelengths range with λ = ∞-456 nm (corresponding to a frequency range 0.0-0.1 a.u) were used in NLO measurements to reveal the dispersion correction contribution to the NLO response for all-trans α,ω-nitro,dimethylamino-hexatriene (Scheme.1). Fig.5, describes the B3LYP/6-31+G* contrasts between the HRS first hyperpolarizability, depolarization ratio and anisotropy factor with the incident light frequency for solvated and isolated all trans α,ω-nitro, dimethylamino-hexatriene. The plot of β_{HRS} *versus* ω for all trans α,ω-nitro, dimethylamino-hexatriene presents a curve, whose peak

corresponding to the predicted resonance region. In the same range, the depolarization ratio displays an accelerating trend and changes drastically.Indeed, DR changes considerably around ω = 0.095 (a.u.), increases with the frequency up to a value close to 4 and then strongly decreases to attain 2 between 0.08 and 0.095 (a.u.), in the 456-506 nm range.

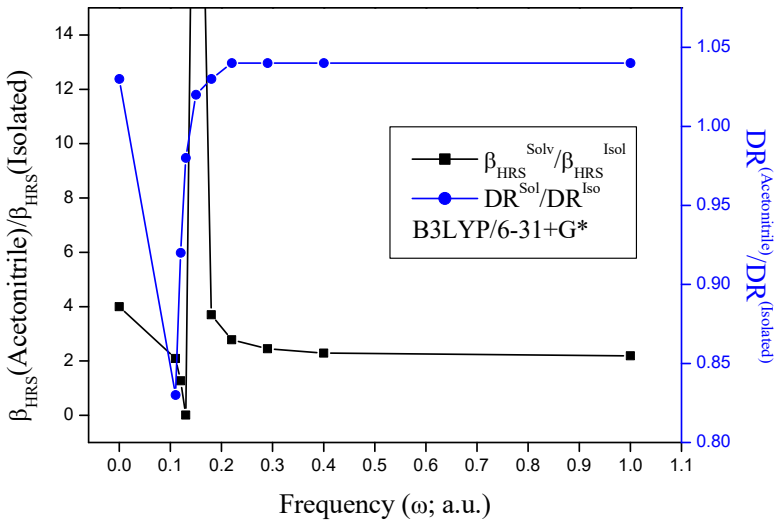

Fig.5. Contrasts between the HRS first hyperpolarizability and depolarization ratio with the frequency for solvated and isolated all trans α,ω-nitro, dimethylamino-hexatriene calculated at B3LYP/6-31+G*.

The comparison of the dynamic β_{HRS} values obtained in vacuum and in acetonitrile reveals that the solvent effect significantly enhances the HRS hyperpolarizabilities of the substituted hexatriene molecule, the dynamic β_{HRS} in acetonitrile increases even more rapidly than in vacuum with increasing the optical wavelengths and the solvent dependent first hyperpolarizability for applied frequencies increases by 20–95%. The frequency dependence hyperpolarizability β_{HRS} in vacuum and acetonitrile tend to follow each other as illustrated by the quantified solvent effect factor $\beta_{HRS}^{(Acetonitrile)}/\beta_{HRS}^{(Isolated)}$ ranging from 2 to 4. For the isolated molecule, the HRS first hyperpolarizability presents a peak at λ = 600 nm whereas the depolarization ratio DR changes considerably in the predicted resonance region between ω= 0.07– 0.08(a.u.) to achieve a maximum value of 4.68 at λ= 651nm, then strongly decreases between λ= 700 nm and 1800 nm to attain the smallest value close 4.00 in this range of

frequency. In addition, since the frequency dependant $DR^{(Acetonitrile)}/DR^{(Isolated)}$ ratio ranges from 0.83 to 1.04, the solvent acetonitrile has little effect on depolarization ratio DR.

3.5 Bond length alternation BLA

The geometries of the substituted all trans-hexatriene were first optimized at B3LYP/ 6-311G* consediring acetonitrile solvent and then, static and dynamic HRS first hyperpolarizability was calculated at the B3LYP/ 6-31+G* level of theory. The variations of bond length alternation (BLA, Å) and the HRS firt hyperpolarizability for the substituted hexatriene molecules (Scheme. 2) are given in Fig. 6.

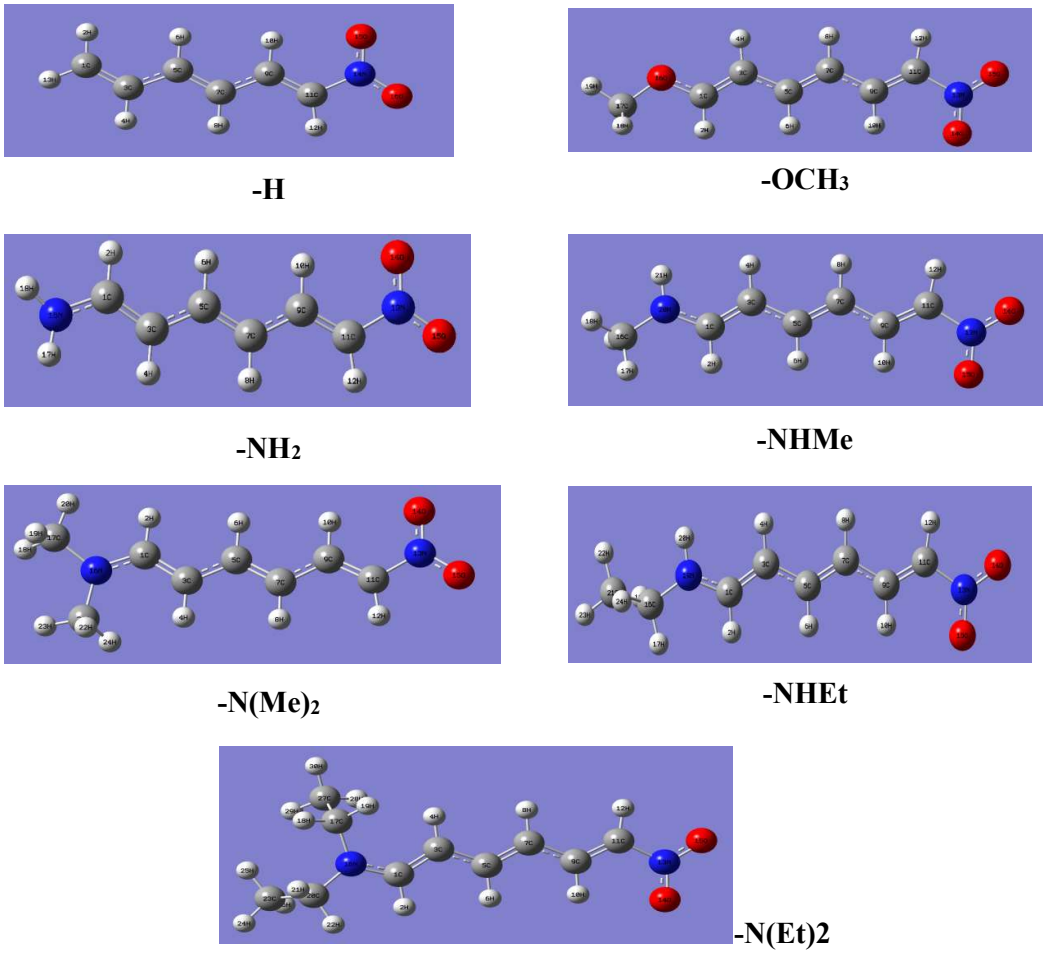

Scheme 3. Illustration of B3LYP/ 6-31+G* optimized substituted hexatriene molecules within NO2/**D** groups (**D**; -H,-OCH_3,-NH_2,-NHMe,-NHEt,-$N(Me)_2$ and -$N(Et)_2$).

It is apparent from Fig.6 that, large and strong substituents -NEt_2 and -NMe_2 groups, make greater structural changes as compared to the small donor groups -OCH_3 ,-CH_3 and -OH. The results first show that the substituents act to reduce the length of the single bonds and to increase the length of the double bonds. As a consequence, the BLA decreases from NO_2/H to NEt_2/ NO_2 by Δ_{BLA} = 0.033 Å. However, the all trans hexatriene present a difference of Δ_{BLA} = 0.042 Å. With regards to the BLA values in the middle and at the end, two different tendencies are found: (i) for the substituted groups -H, -CH_3, -OCH_3, -OH, -NHOH, -NH_2, -$NHNH_2$, -NHMe the BLA increases when going from the middle to the end of the molecules. An increase ranging between 0.001 and 0.012Å in BLA is observed. (ii) In the case of very strong substituted donor (-NHEt, -$N(Me_2)$, -$N(Et_{(2)}$ a decrease of 0.002Å to 0.003Å in BLA takes place from the middle to the end. Compound (11) with –$N(Et)_2$ donor group leads to the smallest BLA value. As regards to the Π-electron donating capacity of the substituted groups, we are able to propose a decreasing classification, relative to β_{HRS} hyperpolarizability. The established order is as follows: NEt_2> NMe_2> NHEt> NHMe > NH_2 > OCH_3 > CH_3 >H.

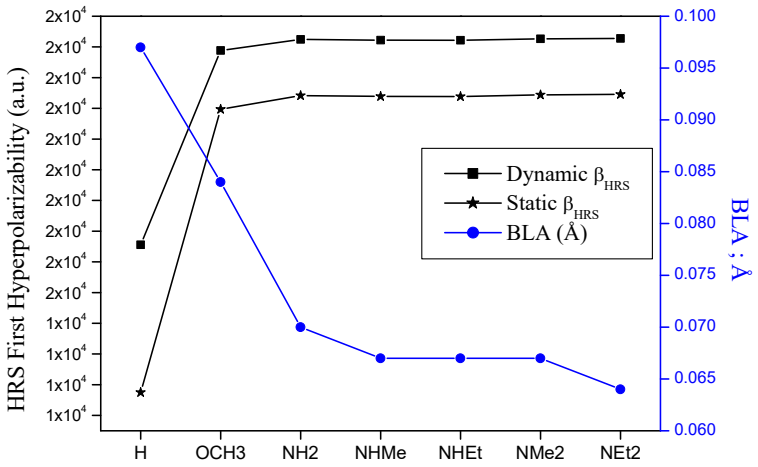

Fig.6. Evolution of the BLA (A˚) and firt hyperpolarizability β_{HRS} for the substituted hexatriene molecules calulated at B3LYP/6-31+G* level.

It can be seen from Fig.6 that, changes in BLA values are generally correlated with the the strengh of the substituted D/A groups. The substituted hexatriene structures become more distorted as indicated by the decreasing BLA values.

Strong Donnor/Acceptor groups will cause a large change in the BLA of the linker and, thereby, have a substantial effect on β_{HRS}. When going from BLA= 0.097Å for (H/NO_2) to BLA=0.064Å of (NEt_2 / NO_2) systems β_{HRS} increases by factors of 2.

4. CONCLUSIONS

The nonlinear optical (NLO) properties of a series of substituted hexatriene is revealed on the basis of HF, DFT and MP2 levels to assess the effects of bridge length, of electron correlation, of frequency dispersion, and of the solvent within the polarizable continuum model, as well as the relationship between the hyper-Rayleigh scattering response and the molecular seize. The main observations are: (i) the calculations indicate that the size and the strengh of substituted groups effects are combined together to determine the hyper-Rayleigh scattering response. In particular, the expanding conjugated system employed to improve the β_{HRS} has been clearly revealed; (ii) as regards to the Π-electron donating capacity of the substituted groups, we are able to propose a decreasing classification, relatively to β_{HRS} hyperpolarizability as follows: NEt_2> NMe_2> NHEt> HHMe >NH_2 >OCH_3> H; (iii) Electron correlation effects are enormous. Among DFT functionals, the B3LYP, B3P86 and M062X are consistent for the estimation of first hyperpolarizabilities (β_{HRS}). However, the MP2 scheme perform quantitatively better regarding the reference SCS-MP2; (iv) The dispersion effects on the β_{HRS} was estimated from the $\beta_{MP2}/\beta_{Method}$ ratios. These dispersion effects are stronger for dialkylamino substituents but remain rather similar among the other compounds; (v) the specific behavior of the HRS first hyperpolarizability with the BLA is significant, When going from BLA= 0.097Å for (H/NO_2) to BLA=0.064Å of (NEt_2 / NO_2) β_{HRS} increases by factors of 2; (vi) A quantitative relationship was established between β_{HRS} and the separation distance $d_{N...N}$.

5. ACKNOWLEDGEMENTS

The author would like to think Professor Benoit Champagne from Namur University -Belgium for his help (Laboratoire de chimie theorique aplliquée.Unité de recherche en chimie physique, théorique et structurale. LCTA-Namur).

6. REFERENCES

[1] Champagne B and. Kirtman B. in Handbook of Advanced Electronic and Photonic Materials and Devices, H. S.Nalwa (Eds.), New York: Academic Press, 2001, pp. 63

[2] Alexander J T L, Elizabeth F. C. D, Stephen C. R, Tobin J. M. Molecular Design Principles for Magneto-Electric Materials: All-Electric Susceptibilities Relevant to Optimal Molecular Chromophores. The Journal of Physical Chemistry C, 2017, 121, (30), 16491 -16500. https://doi.org/10.1021/acs.jpcc.7b04307

[3] Jialei L, Canbin O, Fuyang H, Wenqing H, Aocheng C. Progress in the enhancement of electro-optic coefficients and orientation stability for organic second-order nonlinear optical materials. Dyes and Pigments, 2020, 181, 108509. https:// doi.org/10.1016/ j.dyepig. 2020. 108509

[4] Diego P, Hélio F. Dos Santos. Computational protocol to predict hyper polarizabilities of large π-conjugated organic push–pull molecules. Organic Electronics, 2016, 28,111–117. https://doi.org/10.1016/j.orgel.2015.10.019

[5] Alexander JT L, Tobin J M. A twist on nonlinear optics: understanding the unique response of π-twisted chromophores. Accounts of Chemical Research, 2019, 52, (5),1428 –1438. https://doi.org/10.1021/acs.accounts.9b00077

[6] Oviedo M B, Ilawe NV, Wong B M. Polarizabilities of π-conjugated chains revisited: Improved results from broken-symmetry range-separated DFT and New CCSD benchmarks. J. Chem. Theory Comput, 2016, 12, (8), 3593–3602. https://doi.org/10.1021/acs.jctc.6b00360

[7] Liu Y, Yuan Y, Tian X, Yuan J, Sun J. Computational design of p-(dimethylamino) benzylidene derived push-pull polyenes with high first-hyperpolarizabilities. Phys. Chem. Chem. Phys, 2020, 22, 5090–5104. https://doi.org/ 10.1039/C9CP05631A

[8] Yanling S, Guochun Y. Non-planar donor–acceptor chiral molecules with large second order optical nonlinearities: 1,1,4,4-Tetracyanobuta-1,3-diene derivatives. J. Phys.Chem A, 2014, 118, (6), 1094–1102. https://doi.org/10.1021/jp4099717

[9] Beverina L, Pagani G A. Π-Conjugated zwitterions as paradigm of donor acceptor building blocks in organic-based materials. Accounts of Chemical Research, 2014, 47, (2), 319–329. https://doi.org/10.1021/ar4000967

[10] Lijuan Z, Dongdong Q, Luyang Z, Chao C, Yongzhong B, Wenjun L.Density Functional Theory Study on Subtriazaporphyrin Derivatives: Dipolar/Octupolar Contribution to the Second-Order Nonlinear Optical Activity. J. Phys. Chem. A, 2012, 116, 10249–10256. http:// dx.doi.org/10.1021/jp3079293

[11] Kaushik H, Prasanta K. N. Effect of alkaline earth metal at the single wall CNT mouth on the electronic structure and second hyperpolarizability. Journal of Theoretical and Computational Chemistry, 2016, 15, (05),1650040.https://doi.org/10.1142/S0219633616500401

[12] Champagne B J, Labidi N S. Second-order nonlinear optical responses of heptahelicene and heptathiahelicene derivatives. Chemical Physics Letters, 2016, 644,195–200. http://dx. doi.org/10.1016/j.cplett.2015.12.008

[13] Meier de Andrade A, Loren Inacio P, Alexandre Camilo Jr. Theoretical investigation of second hyperpolarizability of trans-polyacetylene: Comparison between experimental and theoretical results for small oligomers. J. Chem. Phys, 2015,143, 244906–7.https://doi.org/10.1063/1.4939083

[14] Himadri C, Giant first hyperpolarizabilities of donor–acceptor substituted graphyne: An ab initio study. Spectrochimica Acta Part A: Molecular and Biomolecular Spectroscopy, 2016, 153, 226–230. http://dx.doi.org/10.1016/j.saa.2015.08.021

[15] Labidi N S. Solvent effect on hyper-rayleigh scattering (HRS) first hyperpolarizability of substituted polyene: part (I). J. Fundam. Appl. Sci, 2021, 13, (3), 1175–1192. http:// dx.doi.org /10.4314/jfas.v13i3.2

[16] Tomasi J, Mennucci B, Ammi R. Quantum mechanical continuum solvation models. Chem. Rev, 2005, 105, (8), 2999–3094. https://doi.org/10.1021/cr9904009

[17] Sekino H, Bartlett R J. Frequency dependent nonlinear optical properties of molecules. J. Chem. Phys, 1986,85,(2), 976–989. https://doi.org/10.1063/1.451255

[18] Van Gisbergen S J A, Snijders J G, Baerends E J. Accurate density functional calculations on frequency-dependent hyperpolarizabilities of small molecules. J. Chem. Phys, 1998, 109, (24), 10657–10668. https://doi.org/ 10.1063/1.477763

[19] Becke A D. Density functional thermochemistry. III. The role of exact exchange. J. Chem.

Phys, 1993, 98, 5648−5652. https://doi.org/10.1063/1.464913

[20] Zhao Y E, Schultz N and Truhlar D G. Exchange-correlation functional with broad accuracy for metallic and nonmetallic compounds, kinetics, and noncovalent interactions. J. Chem. Phys, 2005, 123, 161103−4. https://doi.org/10.1063/1.2126975

[21] Iikura H, Tsuneda T, Yanai T, Hirao K. A long-range correction scheme for generalized gradient-approximation exchange functionals. J. Chem. Phys, 2001,115, 3540 − 3544. https :// doi.org/10.1063/1.1383587

[22] Yanai T, Tew D P and Handy N C. A new hybrid exchange–correlation functional using the coulomb-attenuating method (CAM-B3LYP). Chem. Phys. Letters, 2004,393, 51−57. https://doi.org/ 10.1016/ j.cplett.2004.06.011

[23] Zhao Y, Truhlar D G. The M06 suite of density functionals for main group thermo-chemistry, thermochemical kinetics, noncovalent interactions, excited states, and transition elements: two new functionals and systematic testing of four M06-class functionals and 12 other functionals. Theor Chem Acc, 2008,120, 215–241. https://doi.org/10.1007/s00214 -007-0310-x

[24] Becke A D. A new mixing of Hartree–Fock and local density-functional theories. J. Chem. Phys, 1993, 98, 1372−1377. https://doi.org/ 10.1063/1.464304

[25] Vosko S J, Wilk L, Nusair M. Accurate spin-dependent electron liquid correlation energies for local spin density calculations: a critical analysis. Can. J. Phys, 1980, 58 1200-1211. https://doi.org/10.1139/p80-159

[26] Plaquet A, Guillaume M, Champagne B, Rougier L, Mançois F,Rodriguez V, Pozzo J L, Lucasse D and Castet F J. Investigation on the second-order nonlinear optical responses in the Keto−Enol equilibrium of anil derivatives. J.Phys.Chem. C, 2008,112, 5638−5645. https://doi.org/10.1021/jp711511t

[27] Castet F, Bogdan E, Plaquet A, Ducasse L, Champagne B, Rodriguez V. Reference molecules for nonlinear optics: A joint experimental and theoretical investigation. J. Chem. Phys, 2012,136, 024506. http://dx.doi.org/10.1063/1.3675848

[28] Yang M, Champagne B. Large off-diagonal contribution to the second-order optical nonlinearities of Λ-shaped molecules. J. Phys. Chem. A, 2003,107, 3942−3951.

https://doi.org/ 10.1021/jp0272567

[29] Frisch M J et al. 2010 Gaussian 09, Revision C. 01.Wallingford CT.

[30] Beverina L, Pagani G. A. Accounts of Chemical Research, 2014,47,319-329. https://doi.org/10.1021/ar4000967

How to cite this article:
Labidi N S. A dft study of hyper-rayleigh scattering (hrs) first hyperpolarizability of substituted polyene: part (ii). J. Fundam. Appl. Sci., 2022, *14(1), 229-251.*